Available online at www.sciencedirect.com
ScienceDirect
Journal of Nuclear Materials 367–370 (2007) 954–959
journal of nuclear materials
www.elsevier.com/locate/jnucmat

The influence of cold-work level on the irradiation creep and swelling of AISI 316 stainless steel irradiated as pressurized tubes in the EBR-II fast reactor

E.R. Gilbert, F.A. Garner *

Pacific Northwest National Laboratory, P.O. Box 999, M/S P8-15 Richland, WA 99354, United States

Abstract

Pressurized tubes of AISI 316 stainless steel irradiated in the P-1 experiment in the EBR-II fast reactor have been measured to determine the dependence of irradiation-induced strains resulting from plastic deformation, irradiation creep, void swelling and precipitation. It is shown that the Soderberg relation predicting no axial creep strains in biaxially-loaded tubes is correct for both plastic and creep strains. Swelling strains are shown to be isotropically distributed both for stress-free and stress-affected swelling, while precipitation strains are somewhat anisotropic in their distribution. When corrected for stress-enhancement of swelling, the derived irradiation creep strains appear to be identical for both annealed and 20% cold-worked specimens, and also for tubes strained by rise to power increases in pressure. For relatively small creep strains it is often difficult to separate the creep and non-creep components of deformation.

1. Introduction

Void swelling and irradiation creep of neutron-irradiated metals are intimately linked phenomena that interact with each other through their response to the local stress state [1]. While void swelling in the absence of stress can be easily measured by various nondestructive and destructive techniques, it is somewhat more difficult to separate irradiation creep strains from non-creep strains such as void swelling, texture-induced recovery, lattice parameter changes resulting from precipitation, plastic strains induced by stresses in excess of the yield strength and the enhancement of swelling by stress. Analysis of irradiation creep experiments is further complicated by the onset of the 'creep cessation' phenomenon at higher swelling levels [1–3], the known anisotropy of precipitation-induced strains at low exposures [1,4] and the suspected anisotropy of strains associated with stress-affected swelling [5,6]. The situation is further complicated by limitations of funding, reactor space and specimen type chosen to conduct irradiation creep experiments.

While creep specimens can take many forms (rods, springs, bent beams, etc.) the favorite form for most creep experiments for the last several decades has been the pressurized tube. Its major advantages are its small size and simplicity of construction and measurement, its nearly constant biaxial stress state even in the presence of substantial swelling,

* Corresponding author. Tel.: +1 509 376 4136; mobile: +1 509 531 2112; fax: +1 509 376 0418.
E-mail address: frank.garner@pnl.gov (F.A. Garner).

0022-3115/$ - see front matter © 2007 Elsevier B.V. All rights reserved.
doi:10.1016/j.jnucmat.2007.03.059

and its lack of need for external mechanical connections.

However, some of its disadvantages are apparent when one attempts to cleanly separate the strains arising from creep and non-creep components. Two general approaches have been taken in the design of creep-swelling experiments and each approach has limitations in this regard. The approach taken in the FFTF–MOTA experiments was to place a series of tubes at different stress levels in an actively-controlled volume where variations in neutron flux and temperature are minimized [7]. The tubes were irradiated, removed and measured, and then returned for further irradiation, repeating the process a number of times. This approach minimizes specimen-to-specimen scatter but does not allow either a clean separation of strains or a determination of the stress-enhancement of swelling.

The approach taken in other experiments conducted in the much smaller EBR-II reactor was to place tubes at different stress levels as close as possible, accepting small variations in flux and temperature, but then to extract and destructively examine each tube after irradiation. This approach allows better separation of strains at the expense of increased data specimen-to-specimen scatter. A similar approach was used by the British in PFR and the French in PHENIX, but the tubes in the French program were welded together into long pins. A review of these studies is published elsewhere [8,9].

Most of the experiments involving irradiations of austenitic stainless steels in FFTF have been published previously [3,8–12]. In a joint US Department of Energy effort involving the Nuclear Energy Research Initiative and Fusion Materials programs, an effort is underway to harvest data and insight from previously unpublished studies conducted decades earlier in the liquid metal reactor program. This first paper of a series addresses selected results of the P-1 experiment.

2. Experimental details

Both 20% cold worked and solution annealed 316 (prepared by heating 20% cold worked cladding for six minutes at 1010 °C) stainless steel cladding were irradiated in the P-1 test. Specimens were manufactured from N-Lot (Heat V87210) and consisted of 25 mm long sections of helium-pressurized cladding as shown in Fig. 1. The fill pressure was verified by measurement of the elastic strain induced during pressurization and also by measurement of the He contained in the specimens after irradiation. The fill gas pressure introduced at room temperature rose as the irradiation temperature was attained, producing mid-wall hoop stresses ranging from 0 to 400 MPa.

Thick-walled capsules, each containing three pressurized tube specimens immersed in static sodium, were stacked and centered in long stainless steel tubes that extended through the EBR-II core. Temperatures were estimated from the calculated gamma heating rate and the thickness of the helium gas gap between the thick-wall capsule and the outer tube. Irradiation temperatures were chosen to span the range 375–577 °C, with uncertainties of ±10 to ±20 °C with increasing target temperatures.

After irradiation the diameter and length changes of the tubes were measured using a laser measurement technique [7]. The end caps were then removed and the density of the tube section determined by an immersion technique accurate to ±0.1%.

3. Results

In Fig. 2 are shown three examples of measurements of length and diameter changes in comparison with one-third of the density conducted on stress-free tubes. Within the accuracy of the measurements it appears that strains arising from stress-free swelling are isotropically distributed, with some indication of possibly small densification in the annealed tubes. This finding suggests that length changes can be used to estimate swelling in stressed tubes where diameter changes include creep strains. In the cold-worked tube, however, the diametral and density strains agree but once swelling begins, the longitudinal strains are measurably larger. This suggests that the anisotropy of precipitation-induced strains reflects the strong texture of cold-worked tubes and resultant orientation of carbide formation [1,4].

Fig. 3 shows the results of a series of annealed tubes irradiated under stress in the range 454–474 °C and 46 dpa to hoop stresses of 95–254 MPa. Note that no comparable specimen is available at 0 MPa. It can be seen that the length changes compare well with one-third of the density changes, indicating that swelling continues to be isotropically distributed, even though swelling is clearly accelerated by stress. The well known Soderberg relationship states that the creep strain developed in biaxial stress states experienced by these tubes will be zero in the axial direction [13], but the

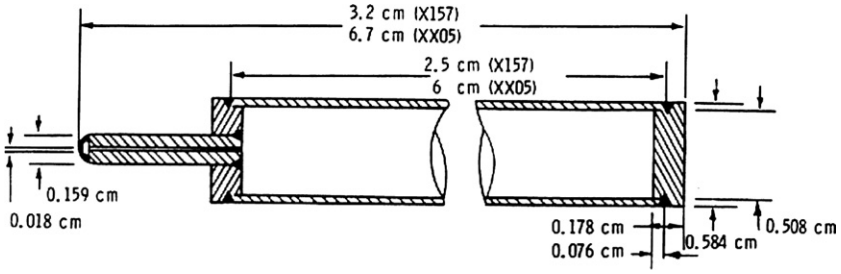

Fig. 1. Pressurized tube specimen design for Test P-1 (EBR-II Subassembly X157) and Test P-5 (EBR-II Subassembly XX05).

distribution of the stress-enhanced portion of swelling has not been well defined in previous studies.

Fig. 4(a) shows, however, that there is a limit to the application of stress and its effect on swelling and creep. Note that at 400 MPa the yield stress of the annealed tube was exceeded when the tube reached 419 °C, producing an immediate plastic strain of ~2% in the diameter but not in the length. This strain produced sufficient cold-working to delay the onset of swelling, however. Densification is not easily visible with such large plastic strains and may be present but overwhelmed by a small amount of swelling. Note that once again the length and density change data agree, indicating that stress-enhanced swelling was isotopic.

Fig. 4(b) shows that the cold worked tubes did not exceed the yield strength at the same nominal irradiation condition and initially densified, developing a low rate of swelling after ~15 dpa. Both annealed and cold-worked tubes thereafter exhibited a similar rate of diameter change, indicating that the eventual creep rates were largely unaffected by the starting condition of the tubes when the swelling is relatively low.

Fig. 5(a) demonstrates the complexity that arises for lower stress levels that marginally exceed the yield stress of annealed steel and produce lower levels of plastic strain. Note that an initial strain of ~0.4% occurs, but the strain decreases thereafter, with some recovery or densification processes occurring. The densification is clearly occurring, reaching ~0.2%, as shown in Fig. 5(c). Swelling becomes dominant only above ~10 dpa.

Fig. 5(b) shows that cold-worked tubes at identical irradiation conditions do not plastically deform but densify initially to about the same level, ~0.2%, but then appear to recover the density loss thereafter, as seen in Fig. 5(c). The length changes also show densification occurring to a lesser extent, but also show that swelling is not significant up to ~22 dpa.

Fig. 6 presents a summary of the stress-normalized diametral creep strains calculated for both annealed and cold-worked tubes, calculated by subtracting the swelling strains from the diameter changes. The large scatter band, especially at lower doses, reflects primarily the strong influence of anisotropic strains associated with precipitation. Note that the creep rates of the annealed and cold-worked steel do not appear to be significantly different once swelling has been removed. The creep coefficient associated with the least squares fit is 1.5×10^{-6} MPa^{-1} dpa^{-1}, somewhat larger than the value of 1×10^{-6} MPa^{-1} dpa^{-1} anticipated in the absence of swelling [1].

4. Discussion

The use of individual pressurized tubes that are irradiated for one period and then destructively examined provides relatively clear separation of the various components of strain, but in order to get different values of dpa or stress one must accept greater data scatter. The scatter arises primarily from three sources. The first source arises from the use of multiple specimens to reach several dose levels, adding specimen-to-specimen variability. The second is particularly important in small reactors with large flux gradients and varying temperature histories, leading to larger uncertainties in irradiation condition. The third source is due to void swelling. Based on other studies it is known that the creep compliance of stainless steels in the absence of swelling is relatively independent of irradiation temperature and dpa rate at 1×10^{-6} MPa^{-1} dpa^{-1}, but when swelling occurs the creep rate is accelerated by an amount proportional to the swelling rate [1]. It is well known that the onset of swelling and the instantaneous swelling rate are very sensitive to every material variable and especially to minor differences in dpa rate and temperature [1]. Thus the swelling-affected creep rate is highly variable in its

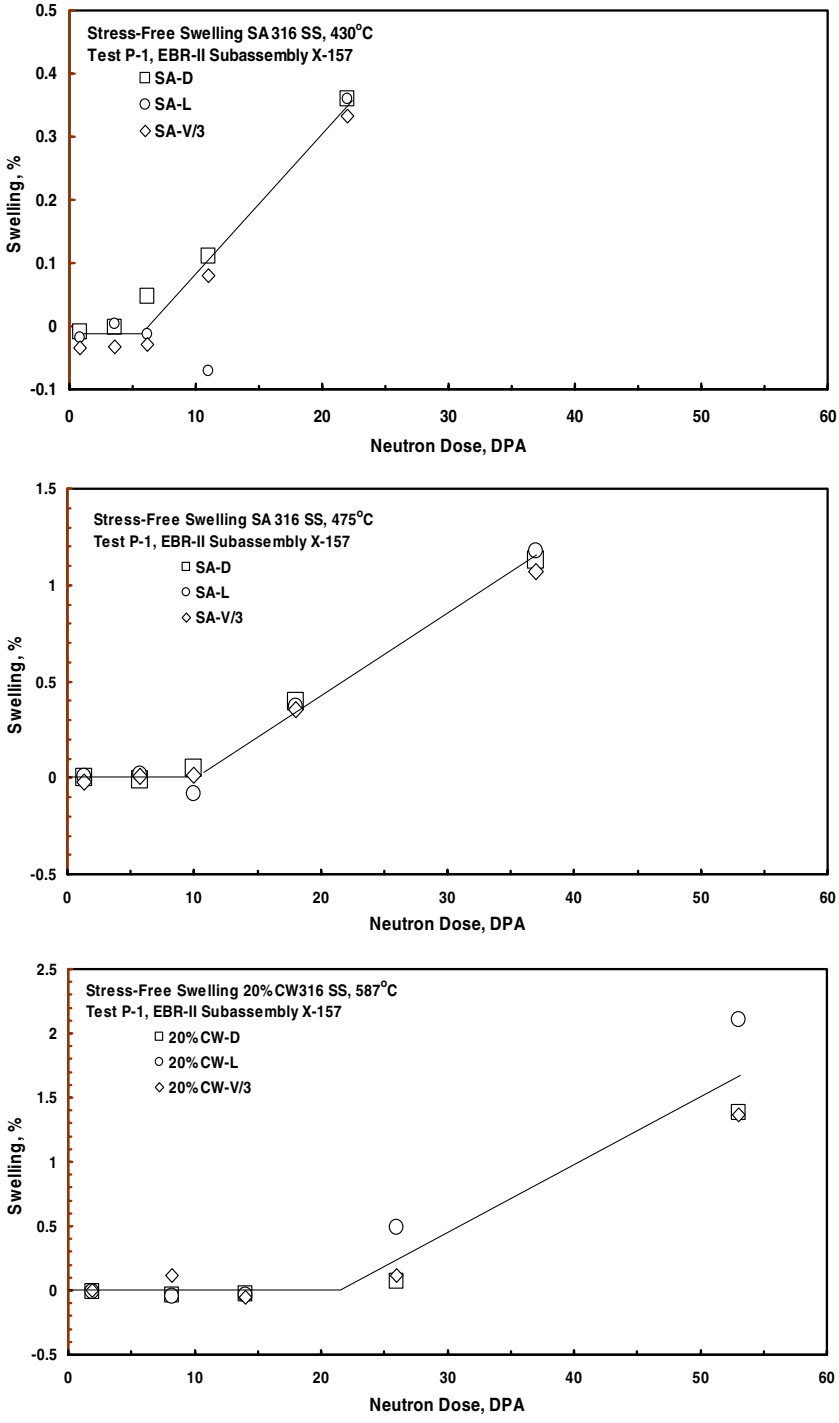

Fig. 2. Comparison of diametral and diameter strains for three sets of stress-free tubes with one-third of the swelling strains as determined by immersion density. In the two sets of annealed tubes all strains appear to be isotropically distributed, but in the cold-worked tubes (bottom) the length strains are larger, probably arising from anisotropy associated with texture induced during drawing of the tube.

response to the local irradiation conditions, introducing additional scatter into the data ensemble.

Much of the reported variation in creep compliance actually results from the inability to separate

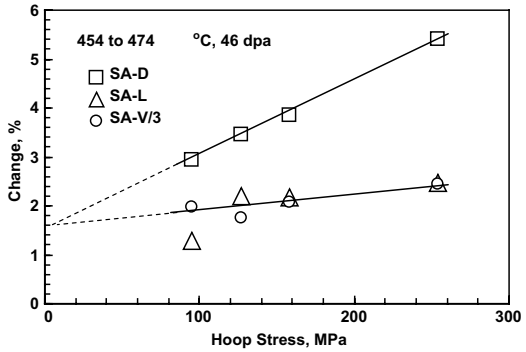

Fig. 3. Comparison of the diameter and length strains of annealed 316 tubes irradiated at 454–474 °C and 46 dpa to hoop stresses of 95–254 MPa, showing stress-affected swelling, isotropy of swelling strains and swelling-enhanced creep.

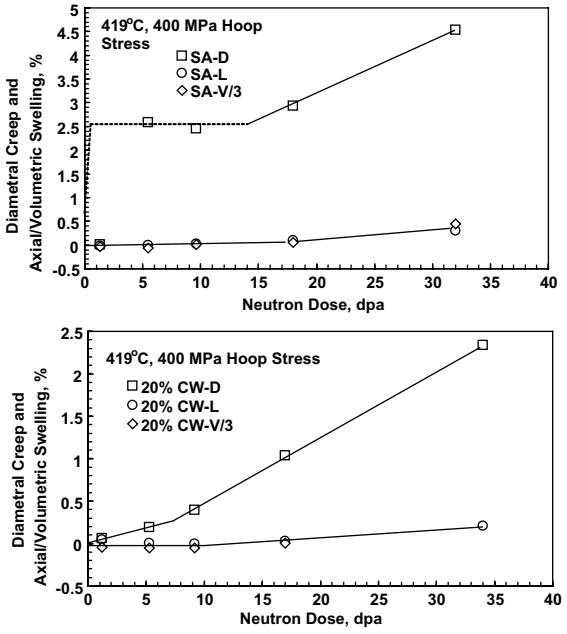

Fig. 4. Comparison of annealed (top) and cold-worked (bottom) tubes irradiated together at 419 °C and 400 MPa hoop stress. The yield strength of the annealed tubes were exceeded during the rise to temperature but the cold-worked tubes did not exceed their yield strength.

the creep strains from the non-creep strains, most of the latter tending to saturate at relatively low doses. In most of the FFTF experiments there was no direct measurement of the stress-induced swelling component, which was incorrectly but necessarily treated as a component of irradiation creep. In most creep experiments the swelling values, whether measured by density change or by dimensional change, include precipitation contributions, introducing

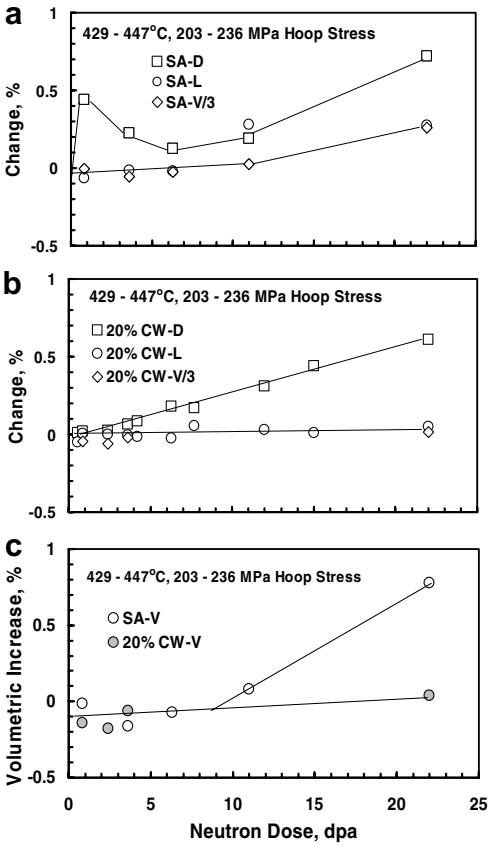

Fig. 5. Comparison of annealed (top) and cold-worked (middle) tubes irradiated at 429-447 °C and 203–236 MPa hoop stress. The yield strength of the annealed tube was slightly exceeded during the rise to temperature but the cold-worked tube was not. The bottom figure compares measured changes in density of both annealed and cold-worked tubes, showing strong densification to ~0.2% early in the irradiation.

additional uncertainties in separation of creep strains.

Within the limitations of this experiment, however, we were able to show that void swelling, both without and with stress, appears to distribute its strains isotropically. It was also shown that both plastically-induced and irradiation creep-induced strains obey the Soderberg relationship, allowing the separate measurement of actual swelling under stress. In addition, it appears that the creep compliance at temperatures below ~500 °C is independent of material starting state, in agreement with earlier studies conducted in FFTF on effects of cold-work level [14,15]. While the scatter is relatively large, especially at relatively low dose levels, the measured creep coefficient is $\sim 1.5 \times 10^{-6}$ MPa^{-1} dpa^{-1}, just slightly larger than the usually accepted creep

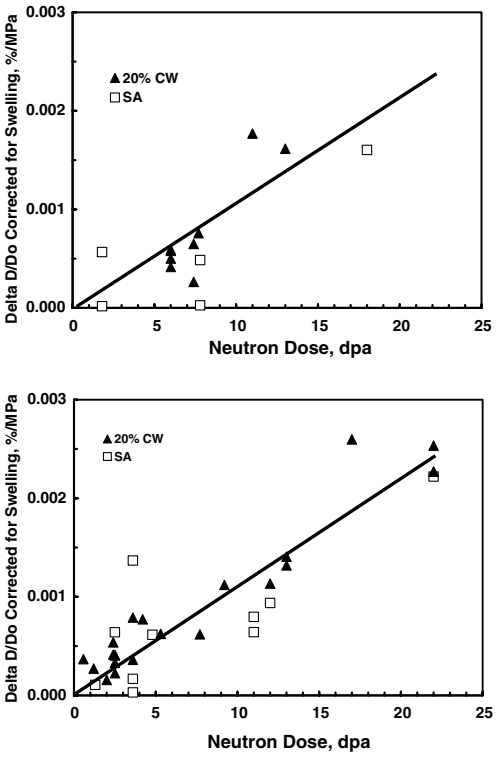

Fig. 6. Diametral strain per unit stress for both annealed and cold-worked tubes after correction for density changes, showing that while scatter can be large at relatively low neutron exposures, the creep strains of annealed and cold-worked tubes are very similar. Data in top figure at 377–447 °C and bottom figure at 477 °C.

compliance of 1×10^{-6} MPa^{-1} dpa^{-1}, reflecting the relatively small and correctly separated amount of swelling in the selected tubes.

5. Conclusions

This experiment has shown that the Soderberg relation predicting no axial creep strains is correct for both plastic and irradiation creep strains measured in AISI 316 stainless steel irradiated in EBR-II. Swelling is shown to be accelerated by stress and its strains are shown to be isotropically distributed both for stress-free and stress-affected swelling, while precipitation strains are somewhat anisotropic in their distribution. When corrected for stress-enhancement of swelling, the derived irradiation creep strains appear to be identical for both annealed and 20% cold-worked specimens.

Acknowledgement

This work was sponsored by the US Department of Energy, Office of Fusion Energy, and the Office of Nuclear Energy, Science and Technology, NERI Project 01-137.

References

[1] F.A. Garner, Chapter 6: Vol. 10A of Materials Science and Technology: A Comprehensive Treatment, VCH Publishers, 1994, pp. 419.
[2] F.A. Garner, D.L. Porter, B.J. Makenas, J. Nucl. Mater. 148 (1987) 279.
[3] M.B. Toloczko, F.A. Garner, J. Nucl. Mater. 212–215 (1994) 509.
[4] F.A. Garner, W.V. Cummings, J.F. Bates, E.R. Gilbert, Hanford Engineering Development Laboratory Report HEDL-TME-78-9, June 1978.
[5] J.F. Bates, W.V. Cummings, E.R. Gilbert, J. Nucl. Mater. 99 (1981) 75.
[6] J.E. Flinn, M.M. Hall, Jr., L.C. Walters, F.A. Garner, J. Nucl. Mater., in preparation.
[7] E.R. Gilbert, B.A. Chin, in: Proceedings of Effects of Radiation on Materials: Tenth Conference, ASTM STP 725, 1981, p. 665.
[8] F.A. Garner, M.B. Toloczko, B. Munro, S. Adaway, J. Standring, in: Proceedings of Effects of Radiation on Materials, 18th International Symposium, ASTM STP 1325, 1999, p. 713.
[9] M.B. Toloczko, F.A. Garner, in: Proceedings of Effects of Radiation on Materials: 19th International Symposium, ASTM STP 1366, 2000, p. 655.
[10] F.A. Garner, M.B. Toloczko, R.J. Puigh, in: Proceedings of Effects of Radiation on Materials: 19th International Symposium, ASTM STP 1366, 2000, p. 667.
[11] M.B. Toloczko, F.A. Garner, J. Nucl. Mater. 212–215 (1994) 509.
[12] F.A. Garner, R.J. Puigh, J. Nucl. Mater. 179–181 (1991) 577.
[13] C.R. Soderberg, Trans. ASME (1963) 737.
[14] F.A. Garner, M.L. Hamilton, C.R. Eiholzer, M.B. Toloczko and A.S. Kumar, in: Proceedings of 16th International Symposium on Effects of Radiation on Materials, ASTM STP 1175, 1992, p. 696.
[15] F.A. Garner, M.L. Hamilton, C.R. Eiholzer, M.B. Toloczko, A.S. Kumar, J. Nucl. Mater. 191–194 (1992) 813.